Calculation of the frequency shifts and damping constant for the Raman modes (A_{1g}, B_1) near the tetragonal-cubic transition in $SrTiO_3$

Ali KİRACI[1], **Hasan Hamit YURTSEVEN**[2,*]
[1]Department of Inter-Curricular Courses, Çankaya University, Ankara, Turkey
[2]Department of Physics, Middle East Technical University, Ankara, Turkey

Abstract: Raman shifts of the soft mode A_{1g} and the B_1 mode are calculated at various pressures at room temperature for the cubic-tetragonal transition ($P_C = 9.5$ GPa) in $SrTiO_3$. This calculation is performed using the observed volume data through the mode Grüneisen parameters of A_{1g} and B_1, which vary with pressure, by fitting to the experimental wavenumbers in this crystalline system. Calculated Raman shifts are then used as order parameters to predict the pressure dependence of the damping constant and the inverse relaxation time for the cubic-tetragonal transition in $SrTiO_3$. Our predictions from the pseudospin-phonon coupling and the energy fluctuation models can be compared with the experimental measurements when available in the literature.

Key words: Raman wavenumber, mode Grüneisen parameter, damping constant, inverse relaxation time, $SrTiO_3$

1. Introduction

$SrTiO_3$ as a model perovskite (ABO_3) exhibits a ferroelastic-antiferrodistortive (AFD) transition from a cubic to a tetragonal structure. Its cubic-tetragonal transition has been the subject of various studies due to its quantum paraelectric behavior at very low temperatures and ferroelastic AFD transition at higher temperatures [1]. Some review papers [2–4] have appeared in the literature about its phase transition. Several experimental and theoretical studies have explained the cubic-tetragonal transition in $SrTiO_3$. Among those studies, acoustic measurements at low temperatures [5–7] and at high pressures [8] and Brillouin [9], Raman [1,10], and X-ray diffraction [1] have been reported, as was also pointed out previously [1].

Raman studies have revealed that there are 7 Raman active modes appearing in the tetragonal phase with the I4/mcm space group, which are not allowed due to symmetry in the cubic phase with the $Pm\bar{3}m$ space group [1,11]. Among those Raman-allowed modes, the two A_{1g} and E_g are the soft modes that drive the antiferrodistortive phase transition in $SrTiO_3$. The 1 (A_{1g} + Eg) and 2 (B_{1g} + E_g) Raman modes in particular have been previously studied experimentally at various high pressures (up to 53 GPa) at constant temperatures for the cubic-tetragonal transition in $SrTiO_3$ [1].

In this study, we calculate the pressure dependence of the Raman wavenumbers of the A_{1g} and B_1 modes from the observed volume data [1] through the mode Grüneisen parameter close to the cubic-tetragonal transition ($P = 9.5$ GPa) at room temperature for $SrTiO_3$. This is performed by fitting to the experimental Raman wavenumbers of the A_{1g} soft mode and the B_1 mode of $SrTiO_3$. From the calculated Raman wavenumbers, the

---

*Correspondence: hamit@metu.edu.tr

pressure dependence of the damping constant and the inverse relaxation time is calculated for this crystal using the pseudospin-phonon coupled (PS) model and the energy fluctuation (EF) model, as we have also studied as examples for $BaTiO_3$ [12] and $SrZrO_3$ [13].

Below, in Section 2, we give an outline of the theory. Section 3 gives our calculations and results. Discussion and conclusions are given in Sections 4 and 5, respectively.

2. Theory

The volume dependence of the Raman wavenumber in $SrTiO_3$ can be defined as the mode Grüneisen parameter:

$$\gamma = -\frac{V}{\omega}\left(\frac{d\omega}{dV}\right). \tag{2.1}$$

When the Raman shifts and the volume V both depend on the pressure at a constant temperature (room temperature), the mode Grüneisen parameter can also depend on the pressure (Eq. (2.1)). If we call it the isothermal mode Grüneisen parameter $\gamma_T(P)$, it can be expressed as

$$\gamma_T(P) = -\frac{V(P)}{\omega(P)}\frac{(\partial\omega/\partial P)_T}{(\partial V/\partial P)_T} \tag{2.2}$$

within the pressure interval where the volume and Raman shifts are obtained. In the case of $SrTiO_3$ as we calculated here, the ratio of the isothermal Grüneisen parameter ($\gamma_T/\gamma_{T,\max}$) of the soft mode A_{1g} varies from about 0.2 to 1.0 in the pressure interval of 10 to 35 GPa. For the B_1 mode, variation of the γ_T is between about –1.5 and 6 within the pressures of $2 < P$ (GPa) < 12.5. From this definition of $\gamma_T(P)$, the Raman shifts can be calculated as given below:

$$\omega_T(P) = \omega_0\exp[-\gamma_T(P)\ln(\frac{V_T(P)}{V_0})], \tag{2.3}$$

where ω_0 and V_0 denote the Raman wavenumber and the volume at room temperature (T = 300 K, P = 0). Thus, by determining $\gamma_T(P)$ and using the volume data at various pressures, the Raman shifts can be calculated in $SrTiO_3$.

Regarding the tetragonal-cubic transition in $SrTiO_3$ ($P_C = 9.5$ GPa), the pressure dependence of the Raman wavenumber can be treated as the order parameter S (tetragonal phase). This then leads to predict the pressure dependence of the damping constant (linewidth) according to the relations

$$\Gamma_{SP} = A'(1-S^2)\ln[\frac{T_C}{T-T_C(1-S^2)}] \tag{2.4}$$

and

$$\Gamma_{SP} = A[\frac{T(1-S^2)}{T-T_C(1-S^2)}]^{1/2}, \tag{2.5}$$

where A' and A are amplitudes, and T_C is the critical temperature for the tetragonal-cubic transition in $SrTiO_3$. The damping constants Γ_{SP} due to the PS model (Eq. (2.4)) and due to the EF model (Eq. (2.5)) were derived by Lahajnar et al. [14] and Schaack and Winterfelt [15] on the basis of the models of Yamada et

al. [16] and Matsushita [17]. Those expressions (Eqs. (2.4) and (2.5)) have been used to explain the mechanism of phase transition in KDP previously [18,19].

Once we predict the pressure dependence of the damping constant (linewidth), activation energy U can be deduced using the following expression [20–22]:

$$\Gamma \cong \Gamma_{vib} + C\exp(-U/k_B T), \tag{2.6}$$

where Γ_{vib} represents the contribution to the damping constant due to vibrations, which can be neglected close to the tetragonal-cubic transition in $SrTiO_3$. This is due to the orientational motion of the BO_6 octahedra in ABO_3 perovskites as in $SrTiO_3$, which causes large bandwidth of the highly energetic vibrational modes (vibrons) in the ordered (ferroelectric) phase. With increasing temperature above the transition, a large reduction of the bandwidth occurs in the disordered (paraelectric) phase of $SrTiO_3$ in particular. Regarding the lattice modes of the A_{1g} soft mode and B_1 mode with the low energies that we study here, variation of the bandwidth (damping constant) with the temperature should not be unexpectedly very large as the vibrations during the phase transition. Then Eq. (2.6) becomes

$$ln\Gamma \cong lnC - U/k_B T, \tag{2.7}$$

with C as a constant and k_B the Boltzmann constant. A plot of $ln\Gamma$ as a function of inverse temperature $(1/T)$ within the pressure range of the tetragonal-cubic transition in $SrTiO_3$ gives rise to the activation energy U, which can be compared with the $k_B T_C$ value at $T = T_C$. Also, using the Raman wavenumber and the damping constant (linewidth), the pressure dependence of the inverse relaxation time (τ^{-1}) can be predicted according to

$$\tau^{-1} = \omega^2/\Gamma \tag{2.8}$$

for the tetragonal-cubic transition in $SrTiO_3$.

3. Calculations and results

The Raman wavenumbers of the soft A_{1g} and B_1 modes were calculated using the observed volume data [1] by determining the isothermal mode Grüneisen parameter γ_T according to Eq. (2.3) at various pressures in the tetragonal phase of $SrTiO_3$. For this determination of γ_T as a function of pressure, we used the observed Raman wavenumbers of these modes with the volume data [1], which were analyzed at various pressures by means of the quadratic function

$$V(P) = c_0 + c_1 P + c_2 P^2, \tag{3.1}$$

where c_0, c_1, and c_2 are constants. These coefficients were determined from our analysis as given in Table 1.

Table 1. Values of the coefficients for the observed volume data [1] with pressure at room temperature according to Eq. (3.1) for the tetragonal-cubic transition in $SrTiO_3$.

Crystal	c_0 (Å^3)	c_1 ($\text{Å}^3/GPa$)	c_2 ($\text{Å}^3/GPa^2$)
$SrTiO_3$	58.98	−0.30	1.72

In order to calculate the Raman wavenumbers of the modes (A_{1g} and B_1), we analyzed the pressure dependence of the observed Raman wavenumbers according to

$$\omega_{obs}(P) = a_0 + a_1 P + a_2 P^2, \tag{3.2}$$

with the coefficients a_0, a_1, and a_2, which we determined, as given in Table 2. We then calculated the Raman wavenumbers (ω_{cal}) of those modes by using the pressure dependence of $\gamma_T/\gamma_{T,\max}$ (A_{1g}) and γ_T (B_1) as determined (Eq. (2.2)) and the observed volume data in Eq. (2.3) by means of the observed wavenumber data (ω_{obs}) [1] according to

Table 2. Values of the coefficients a_0, a_1, and a_2 for the observed wavenumbers [1] with pressure for the Raman modes of A_{1g} and B_1 according to Eq. (3.2). The fitting parameters of b_0, b_1, and b_2 (Eq. (3.2)) are also given here for the two modes studied for the tetragonal-cubic transition in $SrTiO_3$.

Raman modes	a_0 (cm^{-1})	a_1 (cm^{-1}/GPa)	a_2 (cm^{-1}/GPa^2)	$b_0 x10^4$ (cm^{-1})	$b_1 x10^2$	b_2 (cm)
A_{1g}	-64.51	10.87	0.127	32.572	96.426	71.37
B_1	237.95	9.50	0.450	-0.119	0.126	-0.027

$$\omega_{obs}(P) = b_0 + b_1\omega_{cal} + b_2\omega_{cal}^2, \tag{3.3}$$

where b_0, b_1, and b_2 are constants that we determined (Table 2). The mode Grüneisen parameter γ_T was normalized with respect to its maximum value ($\gamma_T/\gamma_{T,\max}$) for the soft mode A_{1g} due to the fact that γ_T diverges as P_C is approached, whereas γ_T for the B_1 mode does not exhibit the anomalous behavior at $P = P_C$ in $SrTiO_3$, as plotted in Figures 1 and 2 for soft mode A_{1g} and the B_1 mode, respectively. Figures 3 and 4 give our calculated Raman wavenumbers of the A_{1g} soft mode and B_1 mode, respectively, as a function of pressure close to the tetragonal-cubic transition ($P_C = 9.5$ GPa) in $SrTiO_3$. The observed Raman wavenumbers [1] of those modes are also shown in these figures.
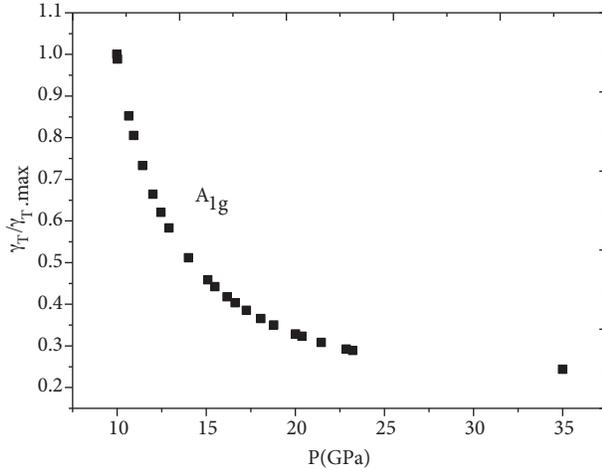
Figure 1. Variation of the isothermal mode Grüneisen parameter (γ_T) (normalized, $\gamma_{T,\max}$ is the maximum γ_T) with pressure for the soft mode A_{1g} close to the tetragonal-cubic transition ($P_C = 9.5$ GPa) in $SrTiO_3$.
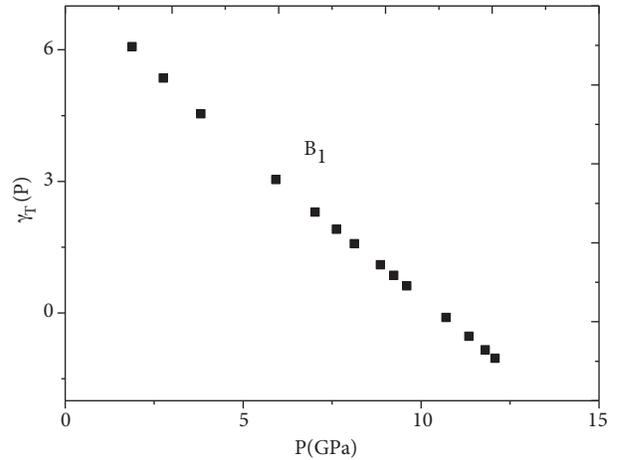
Figure 2. Variation of the isothermal mode Grüneisen parameter (γ_T) with pressure for the B_1 mode close to the tetragonal-cubic transition ($P_C = 9.5$ GPa) in $SrTiO_3$.

The Raman wavenumbers calculated for the soft mode A_{1g} and B_1 mode were then used to evaluate the pressure dependence of the damping constant Γ for the PS model (Eq. (2.4)) and the EF model (Eq. (2.5)) by assuming that the Raman wavenumber can be considered as the order parameter S in the tetragonal phase ($P < P_C$) of $SrTiO_3$. Since the order parameter S varies from 0 (cubic phase) to 1 (tetragonal phase), the Raman
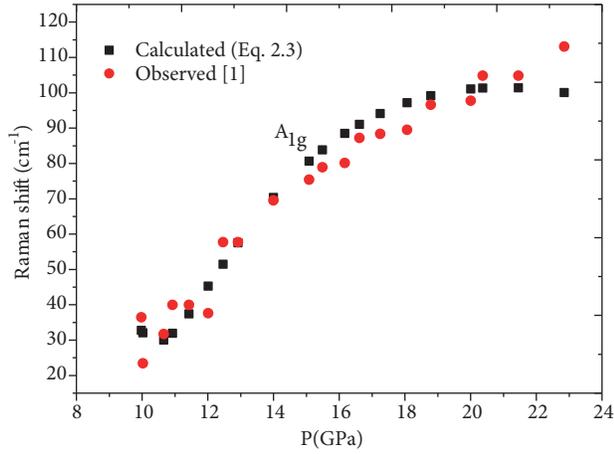
Figure 3. Raman shifts calculated for the soft mode A_{1g} as a function of pressure according to Eq. (2.3) through Eq. (3.3) using the observed volume data [1] for the tetragonal-cubic transition ($P_C = 9.5$ GPa) in $SrTiO_3$. The observed Raman shifts [1] are also shown here.
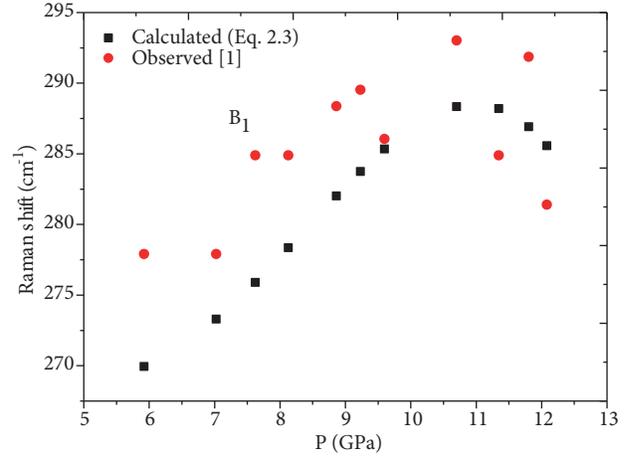
Figure 4. Raman shifts calculated for the B_1 mode as a function of pressure according to Eq. (2.3) through Eq. (3.3) using the observed volume data [1] for the tetragonal-cubic transition ($P_C = 9.5$ GPa) in $SrTiO_3$. The observed Raman shifts [1] are also shown here.

wavenumber of the soft mode was normalized (ω/ω_{max}) with respect to the maximum frequency (ω_{max}). The damping constant Γ was then predicted from ω/ω_{max} as a function of pressure for both models studied. We plot in Figures 5 and 6 our calculated damping constants Γ for the A_{1g} soft mode and the B_1 mode, respectively, using both models (PS model and EF model) as a function of pressure close to the tetragonal-cubic transition ($P_C = 9.5$ GPa) in $SrTiO_3$.
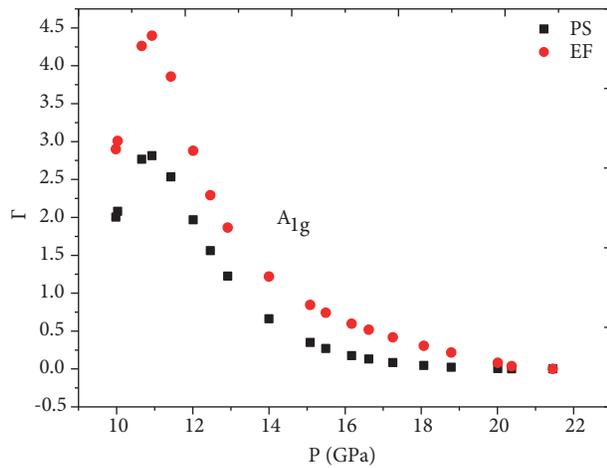
Figure 5. Damping constant (Γ) calculated for the soft mode A_{1g} as a function of pressure using the pseudospin-phonon coupled (PS) model and the energy fluctuation (EF) model according to Eqs. (2.4) and (2.5), respectively, for the tetragonal-cubic transition ($P_C = 9.5$ GPa) in $SrTiO_3$.
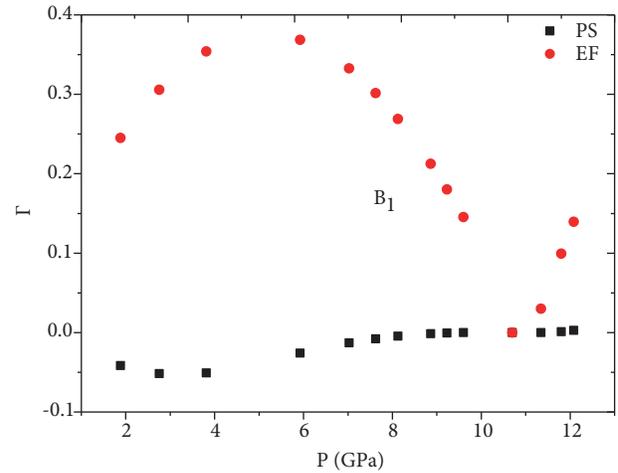
Figure 6. Damping constant (Γ) calculated for the B_1 mode as a function of pressure using the pseudospin-phonon coupled (PS) model and the energy fluctuation (EF) model according to Eqs. (2.4) and (2.5), respectively, for the tetragonal-cubic transition ($P_C = 9.5$ GPa) in $SrTiO_3$.

Using the pressure dependence of the Raman wavenumbers (ω/ω_{max}) and the damping constant (Γ/Γ_{max}) as normalized with the maximum values, we then predicted the inverse relaxation time (τ^{-1}) of the A_{1g} soft mode and the B_1 mode according to Eq. (2.8) as a function of pressure close to the tetragonal-cubic transition in $SrTiO_3$, as plotted in Figures 7 and 8 due to both models (PS and EF) studied. Finally, within the pressure interval corresponding to the temperature range in the T-P phase diagram [1], we extracted the values of the activation energy U according to Eq. (2.7). This was done for the pressure interval of 11.4–18.1 GPa for the soft mode A_{1g} and the two pressure intervals of 1.9–12.1 GPa and 10.7–12.1 GPa as studied for the damping constant Γ using the predictions of the PS model and the EF model, respectively. Our $ln\Gamma$ against T plots (Eq. (2.7)) of the A_{1g} soft mode are given for both models (PS and EF) in Figures 9 and 10, respectively. Within the pressure intervals, values of the activation energy U that we deduced for both models and also the $k_B T_C$ values are given in Table 3. For the B_1 mode, the predicted values of the damping constant Γ were not adequate for the PS model in the pressure region of 10.7–12.1 GPa so that we extracted the activation energy for the 1.9–12.1 GPa pressure interval using the EF model only, as also given in Table 3.
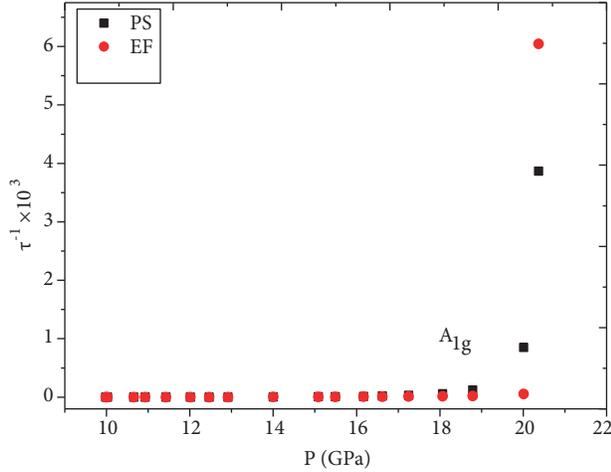
Figure 7. The inverse relaxation time (τ^{-1}) calculated for the soft mode A_{1g} as a function of pressure using the pseudospin-phonon coupled (PS) model and the energy fluctuation (EF) model according to Eq. (2.8) for the tetragonal-cubic transition (P_C = 9.5 GPa) in $SrTiO_3$.
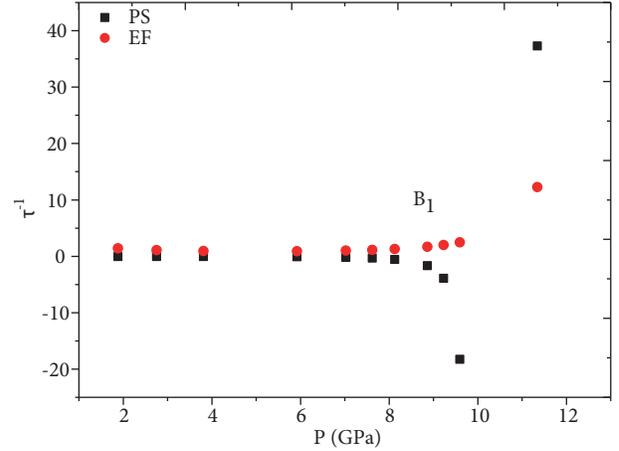
Figure 8. The inverse relaxation time (τ^{-1}) calculated for the B_1 mode as a function of pressure using the pseudospin-phonon coupled (PS) model and the energy fluctuation (EF) model according to Eq. (2.8) for the tetragonal-cubic transition (P_C = 9.5 GPa) in $SrTiO_3$.

Table 3. Values of the activation energy (U) deduced for both models (pseudospin-phonon coupled model - PS and energy fluctuation model - EF) according to Eq. (2.7) in the pressure intervals indicated for the tetragonal-cubic transition in $SrTiO_3$.

Raman modes	P_C (GPa)	T_C (K)	U (meV) PS	U (meV) EF	P (GPa)	$k_B T_C$ (meV)
A_{1g}	9.5	288.0	–420	–253	11.4–18.1	25
B_1			-	395	1.9–12.1	

4. Discussion

Pressure dependences of the Raman wavenumbers of the soft mode A_{1g} and the B_1 mode were calculated using the observed volume data [1] for the tetragonal-cubic transition in $SrTiO_3$. For this calculation of the Raman
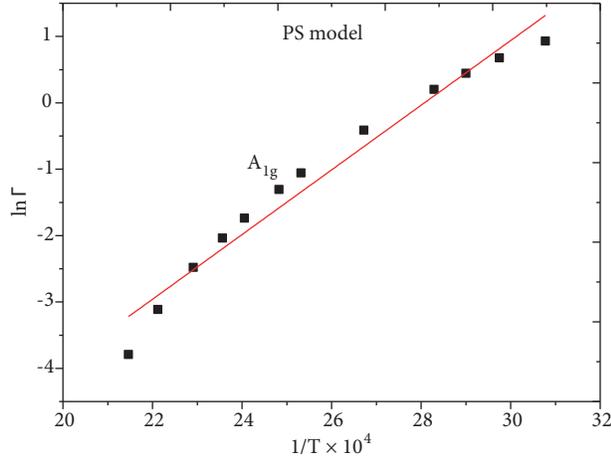
Figure 9. Variation of $ln\Gamma$ with inverse temperature for the soft mode A$_{1g}$ according to Eq. (2.7) using the pseudospin-phonon coupled (PS) model within the pressure range of 11.4–18.1 GPa for the tetragonal-cubic transition in SrTiO$_3$.
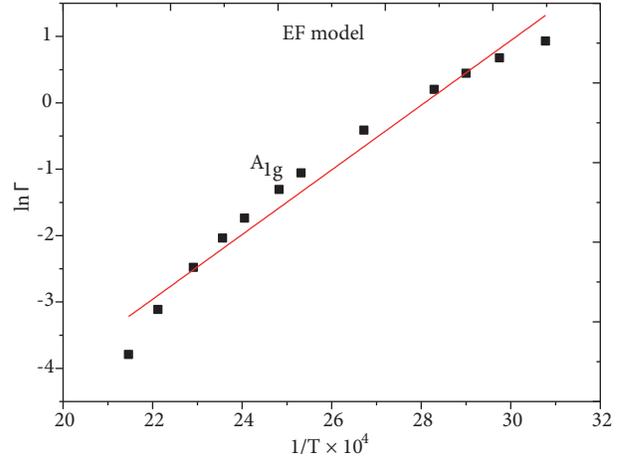
Figure 10. Variation of $ln\Gamma$ with temperature for the soft mode A$_{1g}$ according to Eq. (2.7) using the energy fluctuation (EF) model within the pressure range of 11.4–18.1 GPa for the tetragonal-cubic transition in SrTiO$_3$.

wavenumbers, the pressure dependences of the mode Grüneisen parameters of the soft mode A$_{1g}$ (Figure 1) and the B$_1$ mode (Figure 2) were determined. The normalized mode Grüneisen parameter ($\gamma_T/\gamma_{T,\max}$) for the soft mode A$_{1g}$ and γ_T for the B$_1$ mode decrease as the pressure increases. This decrease is anomalous for the soft mode A$_{1g}$, which diverges as the critical pressure (P$_C$ = 9.5 GPa) is approached (Figure 1), whereas for the B$_1$ mode a smooth (linear) decrease occurs with increasing pressure (Figure 2) for the tetragonal-cubic transition in SrTiO$_3$. This divergence behavior of the $\gamma_T/\gamma_{T,\max}$ for the soft mode A$_{1g}$ at the critical pressure (P$_C$ = 9.5 GPa) is rather unusual as compared to the soft mode A$_1$ (1TO) with the value of its mode Grüneisen parameter –4.7 [23] and –4 ± 0.5 [24] at P$_C$ = 12.1 GPa (at room temperature) in PbTiO$_3$. Also, our value of $\gamma_T \cong$ 0.7 for the B$_1$ mode at P$_C$ = 9.5 GPa of SrTiO$_3$ can be compared with the values of –0.41 [23] and –0.44 ± 0.09 [24] of the B$_1$ + E mode for the cubic-tetragonal transition at P$_C$ = 12.1 GPa (at room temperature) in PbTiO$_3$. Our predictions for the $\gamma_T/\gamma_{T,\max}$ of the A$_{1g}$ soft mode and γ_T value of the B$_1$ mode for SrTiO$_3$ can also be compared with those values when available in the literature.

The Raman wavenumbers of the soft mode A$_{1g}$ were then calculated using the observed volume data [1] by means of the pressure dependence of the $\gamma_T/\gamma_{T,\max}$ (Figure 1) according to Eq. (2.3), which was fitted (Eq. (3.3)) to the experimental wavenumber data [1], as shown in Figure 3. As the observed Raman shifts [1] increase with pressure, our calculated values saturate at about 20 GPa (Figure 3) according to Eq. (2.3). This difference between the observed and calculated Raman shifts may be due to the ratio of the mode Grüneisen parameter $\gamma_T/\gamma_{T,\max}$ for the A$_{1g}$ mode, which is almost independent of the pressure above about 20 GPa (Figure 1). Since below 20 GPa $\gamma_T/\gamma_{T,\max}$ varies rapidly with the pressure (Figure 1), as the observed volume [1] decreases correspondingly the Raman shifts increase with increasing pressure according to Eq. (2.3), as observed experimentally [1]. For the B$_1$ mode the calculated Raman wavenumbers (Eq. (2.3)) disagreed with the observed wavenumbers [1] when Eq. (3.3) was fitted with the coefficients determined (Table 2), although the Raman shifts increase with increasing pressure up to about 11 GPa as observed experimentally (Figure 4). Above 11 GPa, with a linear decrease of γ_T (Figure 2), a decrease in the observed volume [1] causes a

decrease in the Raman shifts of the B_1 mode with increasing pressure according to Eq. (2.3), as also observed experimentally (Figure 4). Disagreement between our calculated and observed [1] Raman shifts of the mode B_1 occurs, which can be due to an almost linear decrease of the mode Grüneisen parameter γ_T for this mode (Figure 2) as compared to a rapid decrease of the $\gamma_T/\gamma_{T,\max}$ for the A_{1g} soft mode (Figure 1) with increasing pressure. Although our calculated Raman shifts of the B_1 mode were fitted to the observed data [1] according to Eq. (3.3), as we also performed for the A_{1g} soft mode, this disagreement also indicates that the A_{1g} soft mode is the driving mechanism for the tetragonal-cubic transition in $SrTiO_3$.

We used the pressure dependence of the Raman wavenumbers of both modes (A_{1g} and B_1) to predict the damping constant Γ by means of the PS model and the EF model according to Eqs. (2.4) and (2.5), as plotted in Figures 5 and 6, respectively. The critical behavior of the damping constant occurs at about 11 GPa for the soft mode A_{1g} due to both models (PS and EF models), as shown in Figure 5, which is not exhibited by the predicted Γ for the B_1 mode (Figure 6) for the tetragonal-cubic transition in $SrTiO_3$. The damping constant of the soft mode A_{1g} peaks at this pressure as predicted by both models (PS and EF). This critical behavior of Γ is consistent with the divergence of the $\gamma_T/\gamma_{T,\max}$ of the A_{1g} mode at nearly 11 GPa (Figure 1) since the damping constant (Γ) is related to the mode Grüneisen parameter (γ_T) through the Raman shifts (ω) as an order parameter.

Regarding the damping constant Γ of the B_1 mode as predicted from the EF model, it decreases rapidly at around P = 11 GPa when it peaks at 6 GPa and then increases with increasing pressure (Figure 6), although its mode Grüneisen parameter (γ_T) decreases smoothly (Figure 2). Correspondingly, Raman shifts of the B_1 mode peak at nearly 11 GPa as calculated from Eq. (2.3) and as observed experimentally (Figure 4). This is not seen for the observed [1] and calculated Raman shifts of the soft mode A_{1g} (Figure 3). This can be clarified by comparing our predicted damping constant Γ of the soft mode A_{1g} and mode B_1 from both models (PS and EF) with the observed linewidths [1].

From the selection of Raman spectra as a function of pressure at room temperature, as observed experimentally [1], while the Raman intensity seems to increase the bandwidths decreases for the soft mode A_{1g} as the pressure increases from 10 to 22 GPa, which agrees with our predictions of the damping constant Γ from both models (Figure 5). On the other hand, the experimental measurements show that the Raman intensity tends to decrease while the bandwidth increases for the B_1 mode for pressures between 2 and 12 GPa [1], which essentially agrees with our Γ values predicted from the PS model and partly agrees above 10 GPa due to the EF model (Figure 6).

The inverse relaxation time (τ^{-1}) of the soft mode A_{1g}, which we calculated (Eq. (2.8)) from both models (PS and EF), diverges at about 20 GPa (Figure 7). This does not indicate a transition occurring since the relaxation time is accompanied with the damping constant (Γ) and the Raman shifts (ω) on the basis of Eq. (2.8). Due to the fact that there is no divergence behavior of the Γ (Figure 5) and ω (Figure 3) of the soft mode A_{1g} at P = 20 GPa, the cubic-tetragonal transition occurs only at P_C = 9.5 GPa (at room temperature) in $SrTiO_3$, as observed experimentally [1]. However, the divergence behavior of the τ^{-1} seems to occur above about P_C = 9.5 GPa as expected for the B_1 mode due to the PS and EF models (Figure 8). This critical behavior is more apparent as predicted from the PS model, whereas the data points for the B_1 mode as calculated from the EF model are not adequate to describe the cubic-tetragonal transition in $SrTiO_3$. However, regarding the pressure dependence of the damping constant Γ of the B_1 mode, the critical behavior is better

described by the EF model than the PS model (Figure 6). This also indicates that regarding Γ and τ^{-1}, one model (PS or EF) is not adequate to describe the cubic-tetragonal transition in SrTiO$_3$. Finally, we extracted the values of the activation energy U from the plots of Figures 9 and 10 as examples using the PS (Eq. (2.4)) and EF (Eq. (2.5)) models, respectively, according to Eq. (2.7) for the soft mode A$_{1g}$ and B$_1$ mode in SrTiO$_3$ (Table 3). Our U values were all negative for the soft mode A$_{1g}$ and we have very large values for the B$_1$ mode above 10 GPa as compared with the $k_B T_C$ value of 25 meV for SrTiO$_3$. In particular, the negative U values for the soft mode A$_{1g}$ may indicate the AFD transition to a tetragonal structure from the cubic phase due to the tilt instabilities at the zone boundary in SrTiO$_3$. In particular, the critical behavior of the mode Grüneisen parameter ($\gamma_T/\gamma_{T,\max}$) (Figure 1) and damping constant Γ (Figure 5) for the soft mode A$_{1g}$, which we calculated using the PS and EF models, indicates a second-order transition from cubic to tetragonal phase in SrTiO$_3$. This is also supported by the pressure dependence of the Raman shifts of this soft mode (Figure 3), which we calculated using the volume data by means of the mode Grüneisen parameter. This also indicates that the soft mode A$_{1g}$ is the driven mechanism of the cubic-tetragonal phase transition in SrTiO$_3$, as stated above.

5. Conclusions

Raman wavenumbers of the soft mode A$_{1g}$ and the B$_1$ mode were calculated as a function of pressure using the observed volume data by means of the mode Grüneisen parameter for the cubic-tetragonal transition in SrTiO$_3$. The pressure dependences of the damping constant and the inverse relaxation time of those modes were also calculated using the PS and EF models for SrTiO$_3$. Our calculations show that the mode Grüneisen parameter decreases rapidly for the soft mode A$_{1g}$, whereas it decreases almost linearly for the B$_1$ mode as the pressure increases. Raman shifts of the soft mode A$_{1g}$ calculated from the volume data agree well with the observed wavenumbers of this mode, which drives the SrTiO$_3$ from the cubic to the tetragonal phase (P$_C$ = 9.5 GPa at room temperature). For the B$_1$ mode, our calculated Raman shifts are not in good agreement with those observed for this transition. Regarding the damping constants of the soft mode A$_{1g}$ as predicted from the PS and EF models, they peak close to the transition pressure (P$_C$ = 9.5 GPa). This critical behavior is predicted by the EF model for the damping constant of the B$_1$ mode. Also, the critical behavior of the inverse relaxation time of the B$_1$ mode is exhibited due to the PS model.

References

[1] Guennou, M.; Bouvier, P.; Kreisel, J.; Machon, D. *Phys. Rev. B* **2010**, *81*, 054115.

[2] Cowley, R. A. *Phil. Trans. Roy. Soc.* **1996**, *354*, 2799-2814.

[3] Hayward, S. A.; Salje, E. K. H. *Phase Transit.* **1999**, *68*, 501-522.

[4] Carpenter, M. A. *Am. Mineral.* **2007**, *92*, 309-327.

[5] Sorge, G.; Schmidt, G.; Hegenbarth, F.; Frenzel, C. *Phys. Status Solidi* **1970**, *37*, K17-K18.

[6] Fossheim, K.; Berre, B. *Phys. Rev. B* **1972**, *5*, 3292-3308.

[7] Okai, B.; Yoshimoto, J. *J. Phys. Soc. Jpn.* **1975**, *39*, 162-165.

[8] Lheureux, D.; Polian, A.; Fischer, M.; Gauthier, M.; Itié, J. P. In *IEEE Ultrasonics Symposium Proceedings*, San Juan, Puerto Rico, 22–24 October 2000; Almar, R., Ed.; Institute of Electrical and Electronics Engineers: New York, NY, USA, 2012, p. 557.

[9] Ishidate, T.; Sasaki, S.; Inoue, K. *High Pressure Research.* **1988**, *1*, 53-65.

[10] Grzechnik, A.; Wolf, G. H.; McMillan, P. F. *J. Raman Spectrosc.* **1997**, *28*, 885-889.

[11] Petzelt, J.; Ostapchuk, T.; Gregora, I.; Rychetský, I.; Hoffmann-Eifert, S.; Pronin, A. V. ; Yuzyuk, Y.; Gorshunov, B. P.; Kamba, S.; Bovtun, V. et al. *Phys. Rev. B* **2001**, *64*, 184111.

[12] Kiraci, A.; Yurtseven, H. *Ferroelectrics* **2012**, *432*, 14-21.

[13] Yurtseven, H.; Kiraci, A. *J. Mol. Struct.* **2017**, *1123*, 51-56.

[14] Lahajnar, G.; Blinc, R.; Zumer, S. *Phys. Cond. Matter* **1974**, *18*, 301-316.

[15] Schaack, G.; Winterfeldt, V. *Ferroelectrics* **1977**, *15*, 35-41.

[16] Yamada, Y.; Mori, N.; Noda, Y. *J. Phys. Soc. Jpn.* **1972**, *32*, 1565-1576.

[17] Matsushita, M. *J. Chem. Phys.* **1976**, *65*, 23-28.

[18] Laulicht, I.; Luknar, N. *Chem. Phys. Lett.* **1977**, *47*, 237-240.

[19] Laulicht, I. *J. Phys. Chem. Solids.* **1978**, *39*, 901-906.

[20] Rakov, A. V. *Opt. Spectrosc.* **1959**, *7*, 128-137.

[21] Bartoli, F. J.; Litovitz, T. A . *J. Chem. Phys.* **1972**, *56*, 413-425.

[22] Fahim, M. A. *Thermochim. Acta* **2000**, *363*, 121-127.

[23] Sanjurjo, J. A.; Lopez-Crus, E.; Burns, G. *Phys. Rev. B* **1983**, *28*, 7260-7268.

[24] Cerdeira, F.; Holzapfel, W. B.; Bauerle, D. *Phys. Rev. B* **1975**, *11*, 1188-1192.